Clays and Clay Minerals, Vol. 21, pp. 229–237. Pergamon Press 1973. Printed in Great Britain

IRON-RICH SAPONITE (FERROUS AND FERRIC FORMS)

NORIHIKO KOHYAMA, SUSUMU SHIMODA and TOSHIO SUDO

Geological and Mineralogical Institute, Faculty of Science, Tokyo University of Education, Tokyo, Japan

(*Received* 18 *October* 1972)

Abstract—Clayey fragments colored deep bluish-green are widely found in glassy rhyolitic tuffs at Oya, Tochigi Prefecture. In room-air the color changes to black or gray within one hour and finally to brown in a few weeks. The fragments are composed of an intimate mixture of two kinds of smectite: a ferrous iron-rich smectite (*IR*) with $b_o = 9{\cdot}300$ Å; and an iron-poor smectite(*IP*) with $b_o = 9{\cdot}030$ Å. Microscopic examination shows a vesicular texture and that *IR* occurs at the core and *IP* at the marginal parts of each vesicle. Analysis by EPMA gave the following structural formulas: *IR*, $(Na_{0{\cdot}60}K_{0{\cdot}04}Ca_{0{\cdot}44})(Mg_{2{\cdot}04}Fe^{2+}_{3{\cdot}98}Al_{0{\cdot}02})(Si_{6{\cdot}36}Al_{1{\cdot}64})O_{20}(OH)_4$; *IP*, $(Na_{0{\cdot}52}K_{0{\cdot}08}Ca_{0{\cdot}26})(Mg_{0{\cdot}90}Fe^{2+}_{0{\cdot}95}Al_{2{\cdot}54})(Si_{7{\cdot}66}Al_{0{\cdot}34})O_{20}(OH)_4$. *IR* has a much larger amount of iron in trioctahedral sites than that found in any earlier data. Acid-dissolution data, infrared absorption spectra, Eh-values, and DTA and TG curves are also given. Ferrous iron in the structure is easily oxidized in room air with loss of protons from the clay hydroxyls and with contraction of the lattice. We call the *IR* before and after oxidation the ferrous and ferric forms, respectively, of iron-rich saponite. They strongly suggest the existence of the iron-analogue of saponite. On exposed weathered surfaces in the field, brown fragments tend to be differentiated into two parts: one light yellow montmorillonite–beidellite; the other a brown incrustation due to hisingerite.

INTRODUCTION

RHYOLITIC glassy tuffs are widely distributed at Oya, Tochigi Prefecture, Japan, and have been used for building stone. Oya-tuffs usually contain many rock fragments of various sizes which have been entirely altered to clay substances. A zone containing especially large fragments alternates regularly in parallel with a zone having no large fragments. The alternation forms a bedding structure. The dip of the bedding plane is nearly 10° and is parallel to that of the shale overlain with Oya-tuffs. High-form quartz and clinoptilolite have been rarely found in the clayey fragments. The fragments show bluish green color on newly cut surfaces of Oya-tuffs in deep caves, and easily turn, in room-air, to black or gray within one hour and finally brown in a few weeks.

This clayey substance was identified and described as iron-rich montmorillonite (Sudo and Ota, 1952); however our studies to date have revealed the detailed mineralogical properties and have shown the need to modify the last conclusion and the nomenclature. The present paper refines the previous study on the basis of the data obtained from some samples selected from many specimens studied. The data from samples 6–1, 9–1 and 10–1 are concerned with properties obtained from the deep bluish-green unoxidized state. The data from samples 6–2, 9–2 and 10–2 are concerned with the brown oxidized parts of samples 6–1, 9–1 and 10–1, respectively.

MINERALOGICAL PROPERTIES OF THE CLAYEY FRAGMENTS

X-ray diffraction data (Table 1) agree with those of smectites. Chemical compositions of the oxidized samples (6–2, 9–2 and 10–2 of Table 2) are like those of montmorillonite–beidellite, though the number of the octahedral cations is intermediate between the dioctahedral and trioctahedral types if the structural formulas are calculated from the bulk chemical composition (Table 2).

The intensity ratio of the (003) to (002) reflections of a dehydrated form is about 5–6, clearly larger than that of the usual dioctahedral smectite. This fact suggests that iron is included in the crystal structure of smectite.

X-ray diffraction has revealed that the present samples are composed of an intimate mixture of two kinds of smectite, because the (06) reflection occurs as a doublet (Table 3). The larger spacing falls in the trioctahedral range, the smaller in the dioctahedral range.

Deep bluish-green unoxidized samples usually have larger amounts of water expelled below 130°C

https://doi.org/10.1346/CCMN.1973.0210405 Published online by Cambridge University Press

Table 1. Spacings of *hk* reflections from mixtures of iron-rich (*IR*) and iron-poor (*IP*) smectites in brown clayey fragments (6–2, 9–2 and 10–2) oxidized in room air

hk	6–2 d(Å)	6–2 I	9–2 d(Å)	9–2 I	10–2 d(Å)	10–2 I
11; 02	4·46	30	4·46	37	4·60 4·48	3 23
13; 20	2·56 2·53	15*b*	2·59 2·53	15b	2·65 2·55	3 13b
22; 04						
31; 15; 24	1·70	5b	1·70	6	1·70	4b
33; 06	1·536 1·501	8 11	1·534 1·503	4 6	1·535 1·501	4 6
26; 40	1·337 1·293	2 3	1·331 1·293	2 2	1·330 1·297	2 2
$a_0 \sin\beta$ (*IR*)	5·35		5·32		5·32	
b_o (*IR*)	9·22		9·20		9·21	
$a_o \sin\beta$ (*IP*)	5·17		5·17		5·18	
b_o (*IP*)	9·01		9·02		9·01	

IR: Iron-rich smectite. *IP*: Iron-poor smectite. $a_o \sin\beta$: calculated from $d(40)$ spacing. b_o: calculated from $d(06)$ spacing. In $d(33;06)$ and $d(26;40)$ spacings, upper values are those of *IR* and lower values those of *IP*.

Table 2. Chemical compositions of unoxidized samples (6–1, 9–1) and oxidized samples (6–2, 9–2, 10–2)

	10–2	9–1	9–2	6–1	6–2
SiO_2	50·03	32·83	46·77	37·02	46·05
TiO_2	tr.	tr.	0·02	0·02	
Al_2O_3	13·94	8·41	12·47	10·90	13·57
Fe_2O_3	9·34	0·93	8·27	0·90	9·15
FeO	2·12	6·75	3·07	7·61	1·56
MnO	0·28	0·20	0·20	0·12	0·14
MgO	3·50	2·58	3·20	3·48	4·32
CaO	1·49	1·38	1·55	1·61	1·99
Na_2O	1·50	1·42	1·50	1·38	1·71
K_2O	tr.	0·21	0·40	0·29	0·36
H_2O^+	5·17	3·46	5·23	4·86	5·17
H_2O^-	12·25	42·04	17·92	33·28	16·00
Total (%)	99·62	100·21	100·60	101·48	100·02
Color of powdered sample	Brown	Blue	Brown	Blue	Brown
Number of octahedral cations*	2·09	2·20	2·08	2·27	2·20

*:When the samples are assumed to be composed of one kind of smectite, the structural formulas are calculated on the basis of $O_{10}(OH)_2$.

than do oxidized samples. Dehydration and decrease of the *b*-parameters occur along with oxidation (from (a–c) of Table 3). The decrease may be due mainly to the smaller radius of ferric with respect to ferrous ions.

Table 3. *b*-parameters and their shrinkages by oxidation

(a) Sample	b_o(Å)	(b) Sample	b_o(Å)	(c) Sample	b_o(Å)
6–1	9·300 9·030	6–1′	9·246 9·012	6–2	9·216 9·006
9–1	9·300 9·048			9–2	9·204 9·018
10–1	9·288 9·036			10–2	9·210 9·012

(a): Unoxidized blue sample. (b): Partially oxidized black sample. (c) Oxidized brown sample. Upper values of each brace are those of iron-rich smectite and lower values are those of iron-poor smectite.

Treatment of the present samples with hydrochloric acid at about 98°C caused dissolution of much of the iron, most of which was dissolved during a short period of an initial dissolution-stage, such as 30 min or 1 hr. At the same time, the larger (06) spacing disappeared. This result suggests that the larger *b*-parameter is that of an iron-rich smectite, the smaller *b*-parameter that of an iron-poor smectite.

Under the microscope, the clayey fragments show a vesicular texture. The core part of each vesicle is dark in color and is composed of aggregates of extremely fine crystals, likely nontronite or saponite. Crystal shades are just visible in the marginal part and show a pale color.

DTA curves (Fig. 1) agree with the usual montmorillonite pattern and show an endothermic peak due to dehydration, an endothermic peak at about 700°C due to dehydroxylation, and a small exothermic peak between 900 and 1000°C. An endothermic peak due to dehydroxylation of nontronite, expected to occur between 400 and 500°C, is scarcely visible.

TG curves (Fig. 1) of the present samples show two steps, due to dehydration and dehydroxylation respectively, which are connected with a gentle slope. It is difficult to estimate from these curves the boundary between the temperature-ranges of dehydration and dehydroxylation. We took the boundary to be 300°C, following the suggestion in the study of the montmorillonite minerals by Ross and Hendricks (1945).

Powders of the present samples were heated in a furnace with a mean heating rate of 10°C per min to coincide with the heating rate of DTA. A part of the powders was taken from the furnace and analyzed chemically for ferrous iron. The results show that most of the ferrous iron has been oxidized in room air below 300°C (Fig. 1).

https://doi.org/10.1346/CCMN.1973.0210405 Published online by Cambridge University Press

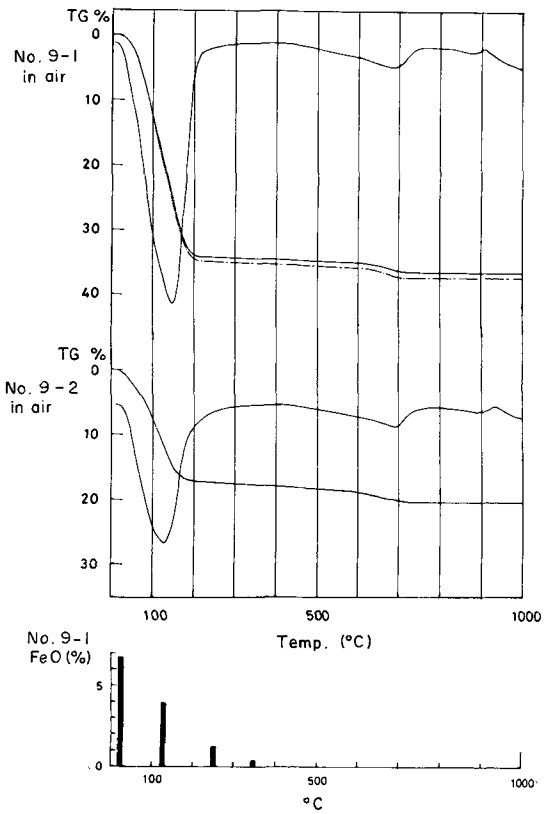


Fig. 1. Upper figure: DTA and TG curves. Mean heating rate is 10°C/min. Sample holder: Platinum. Dotted line is a correction curve with an increase of weight due to oxidation of ferrous iron. Lower figure: Rate of oxidation of ferrous iron caused by heating in room air with mean heating rate of 10°C/min.

The i.r. absorption spectrum of the oxidized sample 6–2 shows absorptions at the following wave numbers: 3610, 3400, 1620, 1122, 1022, 915, 878, 798, 724, 670, 616, 514 and 455 cm^{-1}. The absorptions are characteristic of montmorillonite–beidellite; the bands between 600 and 700 cm^{-1} are considered to arise from the trioctahedral smectite.

It is shown by means of an oxygen-meter that the present samples sorb large amounts of oxygen when oxidized in room air (Fig. 2).

Eh-values of aqueous suspensions of the present samples show a reducing condition for the unoxidized forms (Table 4).

The Mössbauer spectra of the unoxidized (6–1), partially oxidized (6–1′) and oxidized (6–2) samples are shown in Fig. 3. It is clearly shown that the peak at about 2·6 mm/sec shifts to the lower velocity side and the intensity decreases with increasing degree of oxidation of the sample.

Table 4. Eh-values

Color of sample	Eh (mV)
blue	−10–0
black	+120–+130
brown	+140–+160

Eh of distilled water used: +170 mV. The tendency of these Eh-values related to all samples from Oya-tuff, including sample 6–1 and 6–2.

The two peaks at about −0·2 mm/sec and 2·6 mm/sec are those of Fe^{2+}, the peaks at about −0·2 mm/sec and 0·8 mm/sec those of Fe^{3+}. The ratios of the peak intensities in each spectrum agree well with the ratio of the amounts of Fe^{2+} and Fe^{3+} from chemical analysis. The values of isomer shift (I.S.) and quadrupole splitting (Q.S.) for these samples are given in Table 5. Q.S. of Fe^{2+} decreases gradually with increasing degree of oxidation. The other I.S. and Q.S. seem to remain unchanged. This suggests that the site symmetry or structural environment for the iron ion is more symmetrical in the oxidized than in the unoxidized state.

Table 5. Mössbauer parameters

	Oxidation state			
	Fe^{2+}		Fe^{3+}	
	I.S. (mm/sec)	Q.S. (mm/sec)	I.S. (mm/sec)	Q.S. (mm/sec)
6–1	1·19	2·86		
6–1′	1·14	2·56	0·35	0·86
6–2	1·14	2·52	0·36	0·96

I.S.: Isomer shift. Q.S.: Quadrupole splitting.

IDENTIFICATION OF TWO KINDS OF SMECTITE IN THE CLAYEY FRAGMENT

Chemical compositions of some microscopic areas in samples 6–2 were analyzed by EPMA using a polished disk and mineral standards such as some garnets and common hornblende. The results are shown in Fig. 4 and Table 6. Iron is given both in ferrous and ferric forms.

If the iron is treated as being wholly ferrous, as in columns (2) of Table 6, the following structural formulas are obtained on the basis of $O_{20}(OH)_4$:

Iron-rich (core) part

$$(Na_{0\cdot60}K_{0\cdot04}Ca_{0\cdot44})(Mg_{2\cdot04}Fe^{2+}_{3\cdot98}Al_{0\cdot02})(Si_{6\cdot36}Al_{1\cdot64})O_{20}(OH)_4. \quad (a)$$

https://doi.org/10.1346/CCMN.1973.0210405 Published online by Cambridge University Press

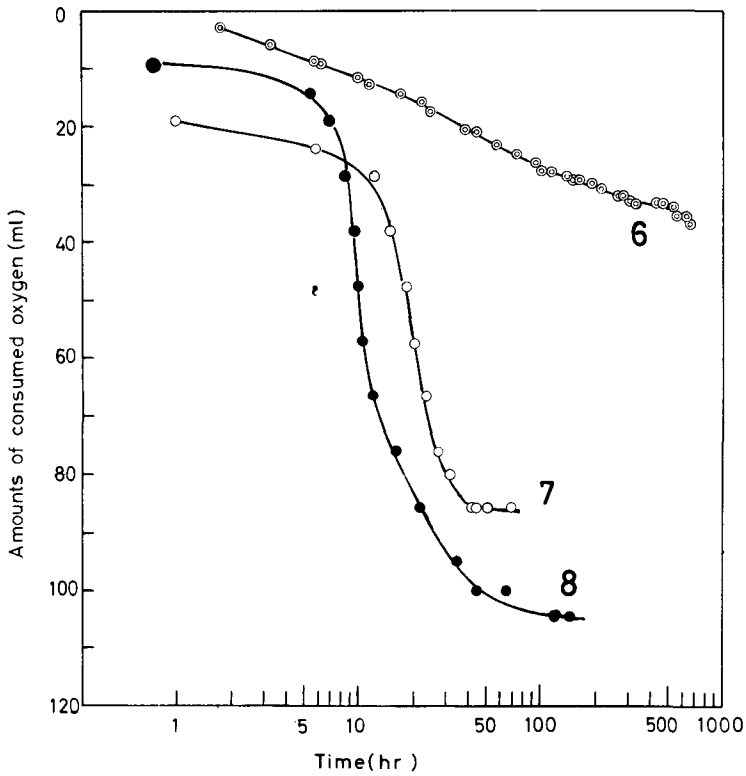


Fig. 2. Variations of the amount of consumed oxygen (ml) by some unoxidized samples (10 g) with the time (hr) of exposure in room air. 6: The present sample (changing from 6–1 (unoxidized) to 6–2 (oxidized) along with time). 7 and 8: These are also the samples from the Oya-tuff but not described in this paper.

Table 6. Chemical analyses by EPMA for sample 6–2

	Core part (A)		Marginal part (B)	
	(1) Ferric form	(2) Ferrous form	(1) Ferric form	(2) Ferrous form
SiO_2	35·5	35·5	49·2	49·2
Al_2O_3	7·9	7·9	15·6	15·6
Fe_2O_3	29·6		8·1	
FeO		26·6		7·3
MgO	7·6	7·6	3·9	3·9
CaO	2·3	2·3	1·5	1·5
Na_2O	1·7	1·7	1·7	1·7
K_2O	0·2	0·2	0·4	0·4
Total (%)	84·8	81·8	80·4	79·6
residual (%)*	15·2	18·2	19·6	20·4

*: This value is considered to be the amount of the interlayer water and the structural water.

Iron-poor (margin) part

$$(Na_{0.52}K_{0.08}Ca_{0.26})(Mg_{0.90}Fe^{2+}_{0.95}Al_{2.52})(Si_{7.66}Al_{0.34})O_{20}(OH)_4. \quad (b)$$

The iron-rich part may be identified as iron-rich saponite and the iron-poor part as montmorillonite–beidellite with medium amounts of Fe and Mg.

If the iron is treated as being wholly ferric, as in columns (1) of Table 6, the following structural formulas are obtained on the basis of $O_{20}(OH)_4$:

Iron-rich (core) part

$$(Na_{0.54}K_{0.04}Ca_{0.40})(Mg_{1.86}Fe^{3+}_{3.04})(Si_{5.84}Al_{1.54}Fe^{3+}_{0.62})O_{20}(OH)_4. \quad (c)$$

https://doi.org/10.1346/CCMN.1973.0210405 Published online by Cambridge University Press

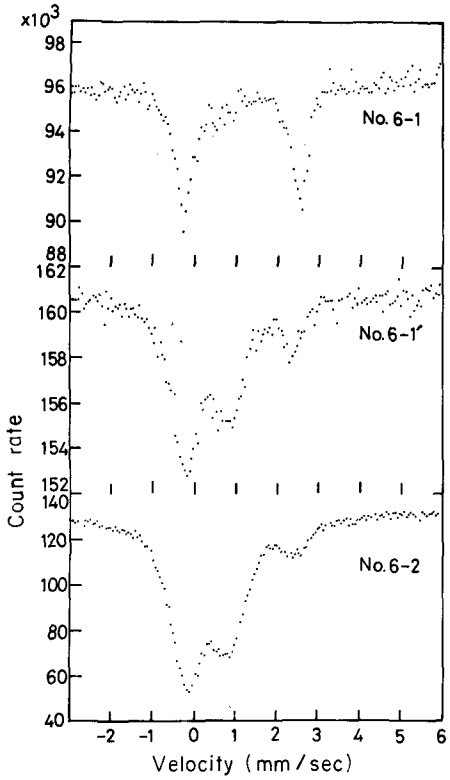


Fig. 3. Mössbauer spectra.

Iron-poor (margin) part

$$(Na_{0.50}K_{0.08}Ca_{0.24})(Mg_{0.88}Fe^{3+}_{0.92}Al_{2.30})(Si_{7.50}Al_{0.50})O_{20}(OH)_4. \quad (d)$$

These formulas are unusual in terms of the deficiency of octahedral cations (considering the unit cell to be trioctahedral), which is due to an unusual amount of tetrahedrally coordinated Fe. Although such behavior is not necessarily improbable because similar defects of lower magnitude have been shown in stevensite, and iron in tetrahedral sites has been demonstrated in cronstedtite, it seems proper to conclude that the iron is present wholly in the ferrous form in these samples of saponite and montmorillonite–beidellite. The structural formula of the ferrous iron–rich saponite is further confirmed by the measurement of structural water in the following paragraphs.

Heat-induced effects of an unoxidized sample (9–1) under various conditions are shown in Table 7. Ferrous iron in the present samples is easily oxidized both at room and higher temperature with sorption of much oxygen from the atmosphere, whereas it is not oxidized in nitrogen or under vacuum of about 10^{0}–10^{-1} Torr either at room temperature or higher.

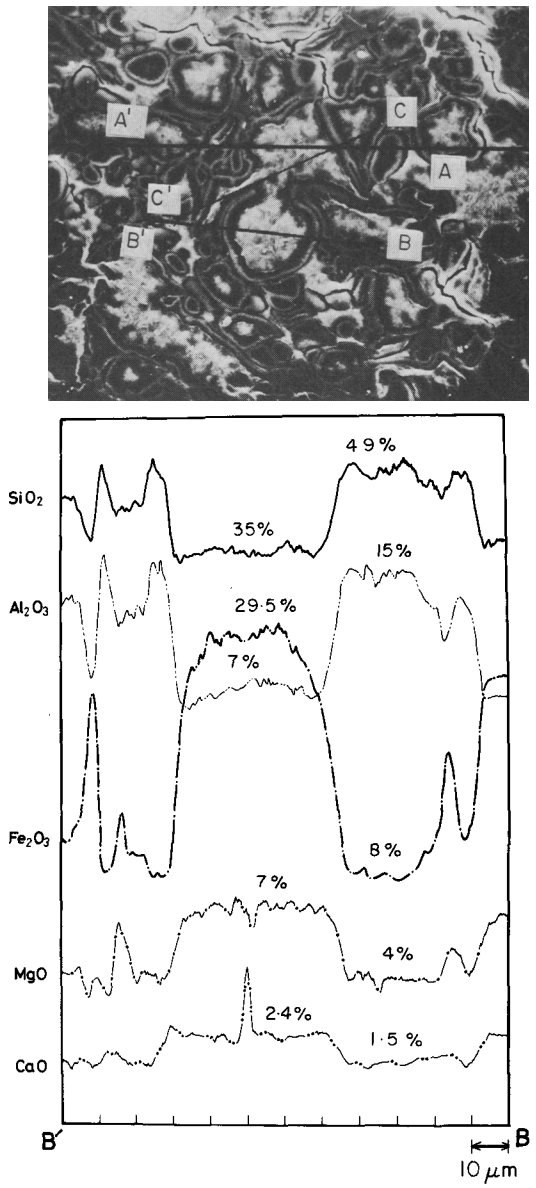


Fig. 4. Upper figure: Secondary electron image of the clayey fragments (6–2). A–A′, B–B′ and C–C′ are traces traversed by electron beams. Lower figure: Changes of chemical compositions along the trace of B–B′ by EPMA.

The weight loss above 300°C, considered to be loss of structural water, was measured carefully by TG or by the weight method on samples 9–1, 9–2, 10–1 and 10–2 in the following four cases: unoxidized samples heated in room air, oxidized samples heated in room air, unoxidized samples heated in vacuum, and oxidized samples heated in vacuum (Table 8). As shown in Table 8, for

https://doi.org/10.1346/CCMN.1973.0210405 Published online by Cambridge University Press

Table 7. (001) spacings and states of iron in various environments

Environment	(001) spacing (Å)	State of iron
Fresh fragments (at about 20°C)	19–21	Fe^{2+} (unox.)
In room air for a few weeks	15	Fe^{3+} (ox.)
In vacuum	10	Fe^{2+} (unox.)
In N_2	15	Fe^{2+} (unox.)
Heated in air (at 250°C)	10	Fe^{3+} (ox.)
Heated in vacuum (at 250°C)	10	Fe^{2+} (unox.)
Heated in vacuum (at 700°C)		Fe^{2+} (unox.)

unox.: unoxidized,
ox.: oxidized.

Table 8. Weight losses above 300°C of samples 9–1, 9–2, 10–1 and 10–2 measured by TGA and/or weight method, in air and in vacuum

Sample	TGA (in air) (%)	TGA (in vacuum) (%)	Weight method (in air) (%)	Weight method (in vacuum) (%)
9–1	3·4	5·8		
9–2	3·5	*		
10–1			3·9	4·6
10–2	4·0		4·0	4·0

9–1: unoxidized sample with mixture of iron-rich and iron-poor smectites of Table 6.
9–2: The same as 9–1 but oxidized one.
10–1: Unoxized sample with mixture of iron-rich and iron-poor smectites of Table 6.
10–2: The same as 10–1 but oxidized one.

oxidized samples these weight losses are close to each other regardless of the different conditions, whereas the weight losses of unoxidized samples heated in room air are clearly smaller than those observed when the unoxidized sample is heated in vacuum, and nearly equal to the losses of the oxidized samples. These values measured under various conditions will be explained by the following calculation.

The mixing ratio of the iron-rich part (iron-rich saponite) and the iron-poor part (montmorillonite–beidellite) is estimated to be 0·2 : 0·8 in sample 6–2. This estimate is based on a comparison of the chemical compositions of the iron-rich and iron-poor parts from the EPMA results (Table 6) with the bulk chemical compositions (Table 2). If the results given in Table 6 for samples 6–2 are used as standards, the mixing ratios of the iron-rich and iron-poor parts of samples 9–2 and 10–2 are 0·2 : 0·8 and 0·15 : 0·85 respectively.

The amount of structural (OH) calculated from the formula of the iron-rich smectite (a) is 3·9 per cent, and from that of the iron–poor smectite(b), 4·6 per cent. When the unoxidized sample is exposed to room air, most of the (OH) ions of formula (a) are converted to oxygen ions as a result of the oxidation of the ferrous ions, because the increased charge due to $3{\cdot}98\ Fe^{2+} \rightarrow 3{\cdot}98\ Fe^{3+}$ is nearly equivalent to that of the $(OH)_4$. Of the $(OH)_4$ of the iron-poor smectite (b), 0·95 (OH) is also converted to oxygen ion by oxidation of ferrous iron. The reactions are as follows:

Iron-rich smectite (A)

$$(Na_{0\cdot60}K_{0\cdot04}Ca_{0\cdot44})(Mg_{2\cdot04}Fe^{2+}_{3\cdot98}Al_{0\cdot02})(Si_{6\cdot36}Al_{1\cdot64})O_{20}(OH)_4 + O_2 \rightarrow (Na_{0\cdot60}K_{0\cdot04}Ca_{0\cdot44})(Mg_{2\cdot04}Fe^{3+}_{3\cdot98}Al_{0\cdot02})(Si_{6\cdot36}Al_{1\cdot64})O_{24} + 2H_2O. \quad (a')$$

Iron-poor smectite (B)

$$(Na_{0\cdot52}K_{0\cdot08}Ca_{0\cdot26})(Mg_{0\cdot90}Fe^{2+}_{0\cdot95}Al_{2\cdot52})(Si_{7\cdot66}Al_{0\cdot34})O_{20}(OH)_4 + 0{\cdot}24\ O_2 \rightarrow (Na_{0\cdot52}K_{0\cdot08}Ca_{0\cdot26})(Mg_{0\cdot90}Fe^{3+}_{0\cdot95}Al_{2\cdot52})(Si_{7\cdot66}Al_{0\cdot34})O_{20\cdot95}(OH)_{3\cdot05} + 0{\cdot}48\ H_2O. \quad (b')$$

The amount of the structural (OH) remaining in (b′) is calculated to be 3·5 per cent; in (a′), zero.

Therefore, if the unit cells are calculated with the iron in the ferrous form on the basis of $O_{20}(OH)_4$, the total amount of the water evolved from the structural (OH) in room air and in vacuum can be calculated as follows:

Sample 9 (9–1 and 9–2);
in vacuum (%) $0{\cdot}2 \times 3{\cdot}9 + 0{\cdot}8 \times 4{\cdot}6 = 4{\cdot}5$,
in room air (%) $0{\cdot}2 \times 0 + 0{\cdot}8 \times 3{\cdot}5 = 2{\cdot}8$.

Sample 10 (10–1 and 10–2);
in vacuum (%) $0{\cdot}15 \times 3{\cdot}9 + 0{\cdot}85 \times 4{\cdot}6 = 4{\cdot}5$,
in room air (%) $0{\cdot}15 \times 0 + 0{\cdot}85 \times 3{\cdot}5 = 3{\cdot}0$.

On the other hand, if the iron is considered to be in the ferric form also on the basis of $O_{20}(OH)_4$, the ferrous iron in the unoxidized sample would be obtained by reduction from formulas (c) and (d), respectively. In this case, the ferrous form would be derived from the primary ferric form. The decrease in positive charge caused by reduction is balanced by an increase of the structural (OH), as follows:

Iron-rich smectite reduced from (c)

$$(Na_{0\cdot54}K_{0\cdot04}Ca_{0\cdot40})(Mg_{1\cdot86}Fe^{2+}_{3\cdot04})(Si_{5\cdot84}Al_{1\cdot54}Fe^{2+}_{0\cdot62})O_{16\cdot34}(OH)_{7\cdot66}. \quad (c')$$

https://doi.org/10.1346/CCMN.1973.0210405 Published online by Cambridge University Press

Iron-poor smectite reduced from (d)

$$(Na_{0.50}K_{0.08}Ca_{0.24})(Mg_{0.88}Fe^{2+}_{0.92}Al_{2.30})(Si_{7.50}Al_{0.50})O_{19.08}(OH)_{4.92}. \quad (d')$$

These formulas have extremely large amounts of structural (OH); calculated values in (c′ and d′) are 7·9 and 5·7 per cent, respectively. Iron-rich smectite (c′) and iron-poor smectite (d′) are oxidized in air to the forms shown by formulas of the structural (OH) expelled as H_2O in air and in vacuum are as follows:

Sample 9 (9–1 and 9–2); in vacuum 6·2%, in air 4·4%.

Sample 10 (10–1 and 10–2); in vacuum 6·0%, in air 4·0%.

The measured values (Table 8) of the structural (OH), expressed as evolved H_2O, are comparatively close to the first case; that is, to the ferrous form of the iron-rich saponite. Therefore, it is concluded that the original form is ferrous on the basis of the quantitative data for structural water.

EARLIER DATA FOR OXIDATION OF FERROUS IRON IN HYDROUS MINERALS

Several concepts have been proposed regarding the oxidation of ferrous iron in hydrous silicate minerals, as follows: (i) reaction between ferrous iron, hydroxyl ion and additional oxygen, as shown in ferrous chamosite by Brindley and Youell (1953) and in oxidized amphiboles by Addison *et al.* (1962a, b); (ii) reaction between ferrous iron and hydroxyl ion without additional oxygen, as shown in biotite by Rimsaite (1967, 1970); (iii) reaction taking place by loss of interlayer cations; and (iv) reaction associated with a reversible conversion of hydroxyl to oxygen ions and subsequent irreversible loss from octahedral sites of ferric ions as iron oxide, as shown in oxidized biotite and vermiculite by Farmer *et al.* (1971).

As mentioned previously, when unoxidized and oxidized samples are heated in vacuum, the structural water evolved from the unoxidized sample is larger than that from an oxidized sample. This difference indicates that some structural (OH) is evidently consumed by the room-temperature oxidation. Oxygen from air also is taken up during the oxidation. It is considered that the oxidation of ferrous iron in the present sample of iron-rich saponite is an example of reaction type (i). The oxidation of the present sample occurs easily at room temperature as well as at elevated temperature, and there is no indication of the formation of iron oxide when the present sample is heated at such elevated temperature.

NOMENCLATURE

The ideal structural formula of saponite has been given as follows:

$$M^{+}_{0.67}(Mg_6)(Si_{7.33}Al_{0.67})O_{20}(OH)_4.$$

Based on the ideal structural formula of smectite, the iron-rich smectite in the present sample is written in the following manner:

$$M^{+}_{0.67}(Mg_2Fe_4{}^{2+})(Si_{7.33}Al_{0.67})O_{20}(OH)_4,$$

which may be called a ferrous iron-which saponite. The formula of the oxidized form, ferric iron-rich saponite, is expressed as follows:

$$M^{+}_{0.67}(Mg_2Fe_4{}^{3+})(Si_{7.33}Al_{0.67})O_{20+4}.$$

"Lembergite" (Sudo, 1943) was defined as an iron-rich saponite (Sudo, 1954), and the ideal structural formula of its ferrous form follows:

$$M^{+}_{0.67}(Mg_3Fe_3{}^{2+})(Si_{7.33}Al_{0.67})O_{20}(OH)_4.$$

These formulas strongly suggest the existence of the iron–analogue of saponite corresponding to the following ideal formula:

$$M^{+}_{0.67}(Fe_6{}^{2+})(Si_{7.33}Al_{0.67})O_{20}(OH)_4.$$

OCCURRENCE OF HISINGERITE

On exposed weathered surfaces in the field, the brown fragments tend to be differentiated into two parts: one is gray montmorillonite–beidellite, and the other is a brown incrustation, which gives a smectite X-ray powder diffraction composed of extremely broad peaks. It is believed therefore that the brown incrustation is hisingerite, a weathered product of iron-rich saponite produced by the following weathering sequence:

Ferrous iron-rich saponite → ferric iron-rich → saponite → hisingerite.

Acknowledgements—The authors wish to thank Dr. Malcolm Ross for his helpful comments, and Dr. H. Hayashi of the National Institute of Industrial Health (Japan) for his valuable suggestions and for use of the i.r. spectrometer. We thank also Prof. H. Sano of Tokyo Metropolitan University for guidance of the study of the Mössbauer effect and Dr. Y. Tanaka of the Shimazu Seisakusho Ltd. for the analysis by EPMA.

https://doi.org/10.1346/CCMN.1973.0210405 Published online by Cambridge University Press

REFERENCES

Addison, C. C., Addison, W. E., Neal G. H. and Sharp, J. H. (1962a) Amphiboles—I. The oxidation of crocidolite: *J. Chem. Soc.* 1468–1471.

Addison, W. E., Neal, G. H. and Sharp, J. H. (1962b) Amphiboles—The kinetics of the oxidation of crocidolite: *J. Chem. Soc.* 1472–1475.

Brindley, G. W. and Youell, R. F. (1953) Ferrous chamosite and ferric chamosite: *Miner. Mag.* **30**, 57–70.

Farmer, V. C., Russell, J. D., MacHardy W. J., Newman, A. C. D., Ahlrichs, J. L. and Rimsaite, J. Y. H. (1971) Evidence for loss of protons and octahedral iron from oxidized biotites and vermiculites: *Miner. Mag.* **38**, 121–137.

Rimsaite, J. (1967) Studies of rock-forming micas: *Geol. Surv., Canada, Bull.*, 149.

Rimsaite, J. (1970) Structural formulae of oxidized and hydroxyl-deficient micas and decomposition of the hydroxyl group: *Contr. Miner. Petrol.* **25**, 225–279.

Ross, C. S. and Hendricks, S. B. (1945) Minerals of the montmorillonite group, their origin and relation to soils and clays: *U.S. Geol. Surv., Prof. Pap.*, **205-B**, 23–79.

Sudo, T. (1943) On some low temperature hydrous silicates found in Japan: *Bull. Chem. Soc. Japan* **18**, 281–329.

Sudo, T. and Ota, S. (1952) An iron-rich variety of montmorillonite found in Oya-ishi: *J. Geol. Soc. Japan* **58**, 487–491.

Sudo, T. (1954) Iron-rich saponite found from Tertiary iron sand beds in Japan: *J. Geol. Soc. Japan* **59**, 18–27.

Résumé—Des fragments argileux d'une couleur vert bleu profond se rencontrent en grand nombre dans des tufs rhyolitiques vitreux à Oya, Préfecture de Tochigi. Dans l'atmosphère ambiante, la couleur passe au noir ou au gris en une heure et finalement au brun en quelques semaines. Les fragments sont constitués par un mélange intime de deux sortes de smectite: une smectite riche en fer ferreux (*IR*) avec $b_o = 9{,}300$ Å, et une smectite pauvre en fer (*IP*) avec $b_o = 9{,}030$ Å. L'examen microscopique montre une texture vésiculaire et indique que *IR* se trouve au centre et *IP* sur les bords de chaque vésicule. L'analyse par EPMA a donné les formules structurales suivantes: *IR*, $(Na_{0,60}K_{0,04}Ca_{0,44})(Mg_{2.04}Fe^{2+}_{3,98}Al_{0,02})(Si_{6,36}Al_{1,64})O_{20}(OM)_4$; *IP*, $(Na_{0,52}K_{0,08}Ca_{0,26})(Mg_{0,90}Fe^{2+}_{0,95}Al_{2,54})(Si_{7,66}Al_{0,34})O_{20}(OM)_4$. *IR* possede une teneur en fer sur les sites trioctaédriques beaucoup plus importante que n'importe laquelle de celles que l'on trouve dans des données plus anciennes. Les résultats de la dissolution acide, des spectres d'absorption infrarouge, des valeurs de E_h et les courbes d'ATD et ATP sont également fournis. Le fer ferreux présent dans le réseau est facilement oxydé à l'air ambiant avec perte de protons à partir des groupes hydroxyle de l'argile et contraction du réseau. Nous appelons *IR* avant et après oxydation les formes ferreuse et ferrique de la saponite riche en fer. Ces formes suggèrent fortement l'existence de l'analogue ferrifère de la saponite. Sur les surfaces exposées à l'altération dans la nature, les fragments bruns tendent à se différencier en deux catégories: une montmorillonite–beidellite jaune clair et une incrustation brune due à la hisingerite.

Kurzreferat—Tief bläulichgrün gefärbte, tonartige Gemengteile werden weithin in glasigen rhyolitischen Tuffen in Oya, Präfektur Tochigi, gefunden. An der Zimmerluft geht die Färbung innerhalb einer Stunde in schwarz oder grau und anschließend in einigen Wochen in braun über. Die Tonanteile bestehen aus einer innigen. Mischung zweier Smectitarten: Einem Fe(2)-reichen Smektit (*IR*) mit $b_0 = 9{,}300$ Å und einem eisennarmen Smectit (*IP*) mit $b_0 = 9{,}030$ Å. Die mikroskopische Untersuchung zeigt, daß eine blasige Struktur vorliegt, und daß *IR* im Kern und *IP* in den randlichen Bereichen jedes Bläschens vorliegen. Die Analyse mit der Elektronenmikrosonde ergab folgende Strukturformeln: *IR*: $(Na_{0.60}K_{0.44})(Mg_{2.04}Fe^{2+}_{3,98}Al_{0.02})(Si_{6.36}Al_{1.64})O_{20}(OH)_4$. *IP*: $(Na_{0.52}K_{0.08}Ca_{0.26})(Mg_{0.90}Fe^{2+}_{0.95}Al_{2.54})(Si_{7.66}Al_{0.34})O_{20}(OH)_4$. *IR* weist einen viel größeren Betrag an Eisen in trioktaedrischer Anordnung auf, als dies bei irgendwelchen früheren Ergebnissen gefunden wurde. Werte zur Säurelöslichkeit, Infrarot-Absorptions-spektren, Eh-Werte, sowie DTA- und TG-Kurven werden ebenfalls mitgeteilt. Zweiwertiges Gittereisen wurde an der Luft leicht oxidiert, wobei Protonenabgabe der Ton-Hydroxylgruppen und Kontraktion des Gitters erfolgte. *IR* vor und nach der Oxidation wird von uns jeweils als Ferro- bzw. Ferriform eines eisenreichen Saponits bezeichnet. Diese Formen machen die Existenz eines FeAnalogons von Saponit sehr wahrscheinlich. An den der Verwitterung ausgesetzten Oberflächen im Gelände neigen die braunen Gemengteile zu einer Trennúng in zwei Anteile: Der eine ist ein hellgelber Montmorillonit–Beidellit, der andere eine braune Verkrustung, die auf Hisingerit zurückgeführt wird.

Резюме — Глинистые секреции ярко сине-зеленого цвета часто встречаются в стекловидных риолитовых туфитах Ойа, префектуры Точиги. В условиях комнатной температуры воздуха в течение одного часа цвет секреций меняется в черный или серый и наконец по истечении нескольких недель в бурый. Секреции состоят из плотной смеси двух смектитов: железистый смектит, богатый железом (*IR*) с $b_0 = 9{,}300$ Å; и смектит с малым содержанием железа (*IP*) с $b_0 = 9{,}030$ Å. Исследование под микроскопом показало, что структура секреций пузырьчатая и, что *IR* встречается в ядре пузырька, в то время как *IP* на гранях каждого пузырька. Ультра микрофотография дала следующие структурные формулы: *IR*: $(Na_{0,60}K_{0,04}Ca_{0,44})(Mg_{2,04}Fe^{2+}_{3,98}Al_{0,02})(Si_{6,36}Al_{1,64})O_{20}(OH)_4$; *IP*: $(Na_{0,52}K_{0,08}Ca_{0,26})(Mg_{0,90}Fe^{2+}_{0,95}Al_{2,54})(Si_{7,66}Al_{0,34})O_{20}$

https://doi.org/10.1346/CCMN.1973.0210405 Published online by Cambridge University Press

$(OH)_4$. *IR* в триоктаэдральных типах имеет значительно более высокое содержание железа, чем указывалось в более ранних работах. Также приводятся данные о кислотном растворении, о инфракрасных спектрах поглощения, о показателе — Eh, о дифференциально термическом анализе и о кривых TG. При комнатной температуре воздуха железистые вкрапления агрегата легко окисляются, что ведет к потере протонов из гидроксилов глины и к сжатию решетки. *IR* до окисления мы называем «ferrous» формой сапонита, богатого железом, а после окисления «ferric» формой того же сапонита. В полевых условиях имеется тенденция разделять бурые секреции на открытых выветрелых поверхностях на две группы: одна — светло-желтая, монтмориллонит-бейделлит; другая — бурая корка образовавшаяся благодаря гизингериту.

https://doi.org/10.1346/CCMN.1973.0210405 Published online by Cambridge University Press